The neuronal pentraxin-2 pathway is an unrecognized target in human neuroblastoma which also offers prognostic value in patients

(Article begins on next page)

10 November 2024

The neuronal pentraxin-2 pathway is an unrecognized target in human neuroblastoma which also offers prognostic value in patients

Alice Bartolini[1], Daniela Di Paolo[2], Alessio Noghero[3], Daniele Murgia[4], Angela R. Sementa[4], Michele Cilli[5], Renata Pasqualini[6,7], Wadih Arap[6,8], Federico Bussolino[3,9], Mirco Ponzoni[2], Fabio Pastorino[2,§] and Serena Marchiò[1,9,§]

[1]Laboratory of Tumor Microenvironment and [3]Laboratory of Vascular Oncology, Candiolo Cancer Institute-IRCCS, Candiolo, Italy; [2]Laboratory of Oncology and [4]Department of Pathology, Istituto G Gaslini, Genova, Italy; [5]Animal Facility, IRCCS Azienda Ospedaliera Universitaria San Martino-IST Istituto Nazionale per la Ricerca sul Cancro, Genova, Italy; [6]University of New Mexico Cancer Center and Divisions of [7]Molecular Medicine, and [8]Hematology/Oncology, Department of Internal Medicine, University of New Mexico School of Medicine, Albuquerque, NM; [9]University of Torino, Department of Oncology, Candiolo, Italy.

[§]F. Pastorino and S. Marchiò contributed equally to this work

Correspondence: Serena Marchiò, Laboratory of Tumor Microenvironment, Candiolo Cancer Institute-IRCCS, S.p. 142 Km 3.95, 10060 Candiolo, Italy: serena.marchio@ircc.it. Fabio Pastorino, Laboratory of Oncology, G Gaslini Institute, Via G Gaslini 5, 16147 Genoa, Italy: fabiopastorino@ospedale-gaslini.ge.it.

Word count: 2775; **Number of Figures**: 4; **Number of Supplementary Figures**: 4

1

Abstract

Neuronal pentraxins (NPTX) and their corresponding receptors (NPTXR) have been studied as synapse-associated proteins in the nervous system, but their role in cancer is largely unknown. By applying a multidisciplinary, high-throughput proteomic approach, we have recently identified a peptide ligand motif for targeted drug delivery to neuroblastoma. Here we report the sequence similarity between this peptide and a conserved portion of the pentraxin domain that is involved in the homo- and hetero-oligomerization of NPTX2 and NPTXR. We show that, in comparison to normal tissues, NPTX2 and NPTXR are overexpressed *in vivo* in mouse models, as well as in human Schwannian stroma-poor, stage IV neuroblastoma. Both proteins are concentrated in the vicinity of tumor blood vessels, with NPTXR also present on neuroblastic tumor cells. *In vivo* targeting of NPTX2 and NPTXR with the selected peptide or with specific antibodies reduces tumor burden in orthotopic mouse models of human neuroblastoma. *In vitro* interference with this ligand/receptor system inhibits the organization of neuroblastoma cells in tumor-like masses in close contact with vascular cells, as well as their adhesion to normal microenvironment-derived cells, suggesting a role in the crosstalk between tumor and normal cells in the early steps of neuroblastoma development. Finally, we show that NPTX2 is a marker of poor prognosis for neuroblastoma patients.

2

Introduction

Neuroblastoma (NB) is the most frequent solid malignancy in the first year of life. Despite recent improvements in treatment, the cure rate for patients with high-risk NB remains poor (1). The genetic nature of this disease has made it difficult to develop targeted therapies: only a few genes have been found mutated, and the occurrence of the corresponding genetic lesions is less than 10%, usually in the 1-3% range (2). Other potential targets have been identified by analysis of copy number variation and epigenetic modifications. However, most of these targets [MYCN, AURKA (3), CHD5 (4), ATRX (5), ARID1A/B (6), ODC (7)] are cytoplasmic or nuclear, making them challenging to target therapeutically. The transmembrane proteins ALK (8) and TrkB (9) are mutated or overexpressed in a substantial number of high-risk NB patients, representing potentially interesting targets. CD19 and GD_2 membrane antigens (10) are being pursued for targeted radiation therapy and nanoparticle-driven drug delivery (11) as well as for antibody-mediated immunotherapy (12), with some success in the treatment and prevention of NB.

While genetic and genomic analyses are powerful approaches for identifying potential therapeutic targets, they do not necessarily reflect the actual amounts, localization, and reciprocal interactions of the gene-encoded proteins. In addition, they provide data only on the tumor cells, without taking into account their microenvironment and tumor/normal tissue interactions, which play critical roles in tumorigenesis (13). Therefore, we have recently developed a multidisciplinary approach to investigate high-risk NB in the context of its native protein architecture, and characterized a set of specific peptide ligand motifs for NB-targeted drug delivery *in vivo* (14).

In the present work, we identify neuronal pentraxin-2 (NPTX2) and its receptor (NPTXR) as a functional ligand/receptor system in NB. Neuronal pentraxins were originally described in the brain as synapse-associated proteins (15), although they are expressed also in few other tissues. Their role as cancer-promoting agents is unknown, with a single recent report showing that NPTX2 is overexpressed in clear cell renal cell carcinoma and induces survival and migration of

3

tumor cells (16). Here we show that NPTX2 and NPTXR are upregulated in NB, and that

blockage of the NPTX2 pathway inhibits the onset of NB by influencing the mutual recognition

between tumor cells and their microenvironment. Finally, we propose the ligand NPTX2 as novel

poor prognostic marker of human NB.

4

Materials and methods

Peptides and antibodies. The previously described HSYWLRS (NB-targeting) and LAKALHA (control) sequences (14) were synthesized by the Institute of Chemistry of Molecular Recognition (National Council of Researches, Milan, Italy) with additional YSHS and GGG sequences at the N- and C-terminal, respectively, and a further C-terminal cysteine residue, resulting in the YSHSHSYWLRSGGGC (TARG) and YSHSLAKALHAGGGC (CTRL) peptide, respectively. The following antibodies were used for (i) *in vivo* studies: anti-NPTX2 (NBP1-50275, Novus Biologicals, Littleton, CO), anti-NPTXR (NPR/B-2, sc-390081, Santa Cruz Biotechnologies, Santa Cruz, CA); (ii) immunostaining: anti-NPTXR (NBP1-86531, Novus Biologicals; HPA001079, Sigma Aldrich, Saint Louis, MO, images in Fig. **1B, S2B** and **S2E**), anti-NPTX2 (PRS4573, Sigma Aldrich), anti-CD146 (EPR3208, Millipore, Vimodrone, Italy), anti-ephrin A1 (sc-911, Santa Cruz Biotechnology), anti-integrin α_{11} (sc-98740, Santa Cruz Biotechnology); (iii) *in vitro* studies: anti-NPTX2 (NBP1-50275), anti-NPTXR (NPR/B-2).

Cell lines and human samples. The human NB-derived cell lines GI-LI-N, HTLA-230, SH-SY5Y and IMR-32 and umbilical vein endothelial cells (HUVECs) were cultured as described (14, 17). Human dermal microvascular endothelial cells (HMECs) were from LGC-Promochem (Sesto San Giovanni, Italy). Human brain vascular pericytes (HBVP) were from ScienCell Research Laboratories (Carlsbad, CA). To obtain fluorescent cells for the *in vitro* assays, GI-LI-N, HTLA-230 and SH-SY5Y cell lines were stably transfected with a plasmid expressing the enhanced green fluorescent protein (pCMS-EGFP, Clontech, Mountain View, CA). Cells were tested and proven negative for mycoplasma contamination and characterized by proliferation, morphology evaluation, and multiplex short tandem repeat profiling. Snap-frozen samples of Schwannian stroma-poor, stage IV NB were provided by BIT. Collection and manipulation of human samples were approved by the Institutional Review Board (IRB). Informed written consent was obtained from each patient in accordance with the Declaration of Helsinki.

5

Mouse models. Athymic (nu/nu) female mice were purchased from Harlan Laboratories (Harlan Italy, S. Pietro al Natisone, Italy) and housed under pathogen-free conditions. Experiments were approved by the Institute Animal Care and Use Committee (IACUC, IRCCS University Hospital San Martino - National Institute for Cancer Research, Genoa, Italy) and by the Italian Ministry of Health. For the orthotopic models, 5-week-old mice were injected into the left adrenal gland with 10^6 NB cells; for the pseudo-metastatic models, 4-week-old mice were injected into the tail vein with 4×10^6 NB cells, as described (14). To evaluate the effect of NPTX2 and NPTXR targeting, GI-LI-N or IMR-32 cells were mixed with CTRL or TARG (100 µM), or with anti-NPTX2 or anti-NPTXR antibody (5 µg/animal) immediately before orthotopic implantation. One month after tumor challenge, mice were killed and tumors explanted.

Data Analysis. Statistical analyses were performed with Prism 5 software (GraphPad, La Jolla, CA). Depending on sample numbers, t-test or Fisher's exact test (two-tailed) were used to compare selected experimental points. Correlation between NPTXR, NPTX2 and VE-cadherin expression with patient outcome was explored using the "R2: microarray analysis and visualization platform" (http://r2.amc.nl) with default parameters for Kaplan-Meier survival graphs. The analysis was performed on the SEQC (SEquencing Quality Control) neuroblastoma project dataset, and the significance was evaluated by Chi-square test.

6

Results and Discussion

We have recently isolated a peptide motif as specific ligand for mouse models of human NB (14). To identify corresponding native ligands, we performed a BLAST analysis against the human and mouse proteomes. Four transmembrane or secreted proteins were retrieved with high homology scores. Of these, ephrin-A1 and α_{11} integrin were not further studied because their expression was barely detectable in NB tissues, as evaluated by IF staining followed by confocal microscopy and quantification (Fig. **S1**, fluorescent pixels $\times$ 10^6). On the other hand, NPTX2 and NPTXR were detected in samples from a panel (n=9) of tumor models obtained by either orthotopic or i.v. injection of NB cell lines (i.e., GI-LI-N, HTLA-230, SH-SY5Y, IMR-32) in athymic mice (Fig. **1A**, fluorescent pixels $\times$ 10^8; Fig. **S2A**, overview of the quantified images; Fig. **S2B**, controls). IF staining of tumor xenografts showed a non-homogeneous localization for these proteins (Fig. **1B**) and, in association with a detailed morphological analysis by IHC, revealed that, while NPTX2 expression is confined to blood vessel-forming and/or surrounding cells (Fig. **1C**, black arrows), NPTXR is present in high amounts also in neuroblastic cells (Fig. **1C**, red arrows). These data are consistent with the *in vitro* expression levels of NPTX2 (low) and NPTXR (medium) in these same NB cell lines, as evaluated by flow cytometry (Fig. **S2C**) and confirmed by immunoblot (Fig. **S2D**). Non-tumor tissues (kidney, adrenal gland, liver) from control animals were largely negative for NPTX2 and NPTXR expression (Fig. **S3**). These findings suggest that the onset and/or progression of NB induce the expression of both ligand and receptor in normal cells of tumor microenvironment, with a concomitant upregulation of the receptor in tumor cells.

NPTX2 and NPTXR represent a peculiar ligand/receptor system whose components share ~50% identity in the overall sequence, and 64% identity in the pentraxin domain where the homology with the targeting peptide is present. Because this domain is responsible for protein-protein interactions leading to functional homo- and hetero-oligomerization (18), we hypothesized that a targeted disruption of such interactions might impact on NB development. To investigate

7

this hypothesis, we first used two mouse models obtained by orthotopic implantation of GI-LI-N and IMR-32 cells into the adrenal glands. We injected cells alone or in the presence of either control (CTRL) or NB-targeting (TARG) peptide, or in the presence of either anti-NPTX2 or anti-NPTXR antibody. After 30 days, mice were killed and organs recovered for tumor burden analysis. We observed a reduction in tumor volume in mice receiving NB cells in the presence of the targeting peptide, as well as of the specific antibodies, compared to cells alone (not shown) or cells plus control peptide (Fig. **1D**). This reduction was significant for all the experimental points in the GI-LI-N model, and for the anti-NPTXR experimental point in the IMR-32 model. A higher affinity/blocking efficiency of the anti-NPTXR monoclonal antibody in comparison to both the peptide and the polyclonal anti-NPTX2 antibody, coupled with slightly different expression levels of the targets, might account for the different significance observed. After treatments, the overall amounts and distribution of both proteins, as well as the vascular architecture, were maintained (Fig. **1E**), suggesting that interference with NPTX2 and NPTXR possibly affects early steps of tumor/normal tissue reciprocal recognition, rather than influencing successive tissue organization during tumor progression.

We therefore evaluated whether *in vitro* blockage of NPTX2 and/or NPTXR would impact the interaction of NB cells with normal cells from the tumor microenvironment. In a first set of experiments, we prepared mixed co-cultures of fluorescently labeled NB cells (GI-LI-N, HTLA-230, SH-SY5Y) and endothelial cells (HUVECs), and grew them in the presence of either CTRL, TARG, anti-NPTX2 or anti-NPTXR. The mixed cells globally reached confluence at the same time in all the experimental conditions; however, their distribution was influenced by the presence of NB-targeting peptide and antibodies. Under control conditions, NB cells were organized in large aggregates reminiscent of tumor masses. In contrast, NPTX2/NPTXR-targeting conditions caused NB cells to become sparse or organized in small clusters. Quantification of highly fluorescent areas (NB cell aggregates) confirmed this redistribution was significant for almost all the experimental points (Fig. **2A**). We investigated whether this effect was related to NPTX2/NPTXR-

8

mediated cell-cell binding, by incubating each fluorescent NB cell line on confluent layers of macrovascular (HUVECs), microvascular (HMECs) or perivascular (HBPV) cells, in either control or NPTX2/NPTXR targeting conditions. Adhesion of NB cells onto macrovascular and microvascular cells was impaired when NPTX2 and NPTXR were targeted; binding to perivascular cells was only slightly affected by interference with the NPTX2/NPTXR pathway (Fig. **2B**). All these microenvironment cells express both NPTX2 and NPTXR; however, NPTXR levels are markedly higher in pericytes (Fig. **S2D-E**), possibly accounting for the weaker inhibition observed. We also evaluated whether NPTX2 and/or NPTXR had a role in NB cell migration towards normal microenvironment cells. For these assays, we chose the SH-SY5Y cell line after extensive characterization of the migratory properties in all NB cell lines (Fig. **S4**). Interestingly, attraction of SH-SY5Y was increased by treatment with either targeting peptide or anti-NPTXR antibody, while interfering with NPTX2 was ineffective (Fig. **2C**). Together, these data show that NPTX2 and NPTXR affect the spatial organization and reciprocal recognition of neuroblasts and normal cells. They demonstrate that, in this setting, (i) the NPTX2/NPTXR pathway has a pro-adhesive effect, (ii) NPTXR, possibly activated by an alternative ligand such as NPTX1 (18), has an anti-migratory effect, and (iii) both functions are reverted by a specific targeting of NPTX2 and/or NPTXR.

Having shown that NPTX2 and NPTXR are potential targets in NB *in vivo* and *in vitro*, we evaluated their expression in human NB samples. The overall tissue distribution of both proteins was similar to that seen in the mouse models, although more background was visible in the staining for NPTX2, due to technical issues (FFPE mouse samples *versus* snap-frozen human specimens) (Fig. **3A**). Notably, in contrast to the high amounts of both NPTX2 and NPTXR detected in NB, undetectable to low expression of these proteins is reported by the Human Protein Atlas (19) for the same normal tissues that we evaluated in mice (Fig. **S5**). These data demonstrate that both proteins are overexpressed in NB in clinical settings.

This finding led us to investigate a possible involvement for either protein during the progression of human NB. For this purpose, we exploited public microarray expression data that we evaluated through the "R2 microarray analysis and visualization platform". Analysis of a large patient dataset (SEQC, n=498) revealed that high levels of NPTX2 strongly correlated with poor overall survival (P = 3.2e-06). Unexpectedly, NPTXR had a different trend, although with lower significance (P = 0.019) (Fig. **3B**). One might speculate a possible explanation for this paradoxical result is that, while NPTX2 localizes prevalently to vascular compartments, NPTXR is expressed also by tumor cells distant from the blood vessels (Fig. **1C** and **E**). It is therefore conceivable that a substantial amount of the receptor binds to an alternative pentraxin ligand (18, 20), with a different biological outcome. Unfortunately, the SEQC dataset reports only a whole-tissue mRNA expression analysis, from which it is impossible to distinguish among the different species of NPTXR. The poor prognostic value of NPTX2 was not a surrogate for endothelial cell content: another endothelial expressed gene, VE-cadherin followed an opposite trend and correlated with good overall survival (P = 6.1e-05) (Fig. **3B**).

In conclusion, we show that NPTX2 and NPTXR mediate tumor/normal cell recognition in NB and that interfering with this ligand/receptor system is a potential approach towards the development of an innovative targeted therapy. We summarize the proposed mechanism in Fig. **4**. Finally, we show that NPTX2 is a novel poor prognosis tumor marker for NB patients.

10

Acknowledgments

11

References

1. Maris JM. Recent advances in neuroblastoma. *New Eng J Med*. 2010;**362**:2202-11.

2. Pugh TJ, Morozova O, Attiyeh EF, Asgharzadeh S, Wei JS, Auclair D, et al. The genetic landscape of high-risk neuroblastoma. *Nat Genet*. 2013;**45**:279-84.

3. Gustafson WC, Meyerowitz JG, Nekritz EA, Chen J, Benes C, Charron E, et al. Drugging MYCN through an allosteric transition in Aurora kinase A. *Cancer Cell*. 2014;**26**:414-27.

4. Koyama H, Zhuang T, Light JE, Kolla V, Higashi M, McGrady PW, et al. Mechanisms of CHD5 Inactivation in neuroblastomas. *Clin Cancer Res*. 2012;**18**:1588-97.

5. Cheung NK, Zhang J, Lu C, Parker M, Bahrami A, Tickoo SK, et al. Association of age at diagnosis and genetic mutations in patients with neuroblastoma. *JAMA*. 2012;**307**:1062-71.

6. Sausen M, Leary RJ, Jones S, Wu J, Reynolds CP, Liu X, et al. Integrated genomic analyses identify ARID1A and ARID1B alterations in the childhood cancer neuroblastoma. *Nat Genet*. 2013;**45**:12-7.

7. Hogarty MD, Norris MD, Davis K, Liu X, Evageliou NF, Hayes CS, et al. ODC1 is a critical determinant of MYCN oncogenesis and a therapeutic target in neuroblastoma. *Cancer Res*. 2008;**68**:9735-45.

8. Bresler SC, Weiser DA, Huwe PJ, Partk JH, Krytska K, Ryles H, et al. ALK Mutations Confer Differential Oncogenic Activation and Sensitivity to ALK Inhibition Therapy in Neuroblastoma. *Cancer Cell*. 2014;**26**:682-94.

9. Brodeur GM, Minturn JE, Ho R, Simpson AM, Iyer R, Varela CR, et al. Trk receptor expression and inhibition in neuroblastomas. *Clin Cancer Res*. 2009;**15**:3244-50.

10. Lee DW, Barrett DM, Mackall C, Orentas R, Grupp SA. The future is now: chimeric antigen receptors as new targeted therapies for childhood cancer. *Clin Cancer Res*. 2012;**18**:2780-90.

11. Pastorino F, Brignole C, Loi M, Di Paolo D, Di Fiore A, Perri P, et al. Nanocarrier-mediated targeting of tumor and tumor vascular cells improves uptake and penetration of drugs into neuroblastoma. *Front Oncol*. 2013;**3**:190.

12. Yu AL, Gilman AL, Ozkaynak MF, London WB, Kreissman SG, Chen HX, et al. Anti-GD2 antibody with GM-CSF, interleukin-2, and isotretinoin for neuroblastoma. *New Engl J Med*. 2010;**363**:1324-34.

13. Marchiò S, Soster M, Cardaci S, Muratore A, Bartolini A, Barone V, et al. A complex of alpha6 integrin and E-cadherin drives liver metastasis of colorectal cancer cells through hepatic angiopoietin-like 6. *EMBO Mol Med*. 2012;**4**:1156-75.

14. Loi M, Di Paolo D, Soster M, Brignole C, Bartolini A, Emionite L, et al. Novel phage display-derived neuroblastoma-targeting peptides potentiate the effect of drug nanocarriers in preclinical settings. *J Control Release*. 2013;**170**:233-41.

15. Hsu YC, Perin MS. Human neuronal pentraxin II (NPTX2): conservation, genomic structure, and chromosomal localization. *Genomics*. 1995;**28**:220-7.

16. von Roemeling CA, Radisky DC, Marlow LA, Cooper SJ, Grebe SK, Anastasiadis PZ, et al. Neuronal pentraxin 2 supports clear cell renal cell carcinoma by activating the AMPA-selective glutamate receptor-4. *Cancer Res*. 2014;**74**:4796-810.

17. Pastorino F, Brignole C, Marimpietri D, Cilli M, Gambini C, Ribatti D, et al. Vascular damage and anti-angiogenic effects of tumor vessel-targeted liposomal chemotherapy. *Cancer Res*. 2003;**63**:7400-9.

18. Dodds DC, Omeis IA, Cushman SJ, Helms JA, Perin MS. Neuronal pentraxin receptor, a novel putative integral membrane pentraxin that interacts with neuronal pentraxin 1 and 2 and taipoxin-associated calcium-binding protein 49. *J Biol Chem*. 1997;**272**:21488-94.

19. Uhlen M, Fagerberg L, Hallstrom BM, Lindskog C, Oksvold P, Mardinoglu A, et al. Proteomics. Tissue-based map of the human proteome. *Science*. 2015;**347**:1260419.

20. Osmand AP, Friedenson B, Gewurz H, Painter RH, Hofmann T, Shelton E. Characterization of C-reactive protein and the complement subcomponent C1t as homologous proteins displaying cyclic pentameric symmetry (pentraxins). *Proc Natl Acad Sci USA*. 1977;**74**:739-43.

13

Figure Legends

Figure 1. NPTX2 and NPTXR are functional markers in experimental mouse models of NB.

NPTX2 and NPTXR were evaluated by IF and IHC in the following tumor samples: **G1-2**, orthotopic GI-LI-N cells (**G1**, primary tumor; **G2**, lymph node metastasis); **H1-4**, i.v. HTLA-230 cells (tumor mass in: **H1**, left ovary; **H2**, right kidney; **H3**, right adrenal gland; **H4**, left adrenal gland); **S1**, orthotopic SH-SY5Y cells, primary tumor; **I1-2**, i.v. IMR-32 cells (tumor mass in: **I1**, bladder; **I2**, right adrenal gland). FFPE tissues were immunostained for NPTX2 and NPTXR. (**A**) Quantification of specific signals by ImageJ; graph bars represent mean ± S.D. from 6 pictures of each sample. (**B**) Representative IF pictures. Anti-NPTXR, HPA001079; nuclei, DAPI. (**C**) Subset of NB tissues IHC-stained and counterstained with hematoxylin. Black arrows, blood vessels; red arrows, tumor cells. (**D-E**) GI-LI-N or IMR-32 cells were implanted into the adrenal gland (n=5 mice *per* group) in the presence of CTRL, TARG, anti-NPTX2 or anti-NPTXR. Tumor volumes were evaluated after 30 days (**D**). Representative IHC staining of samples from the GI-LI-N model; arrows as in Fig. **1C** (**E**). The experiment was performed twice with similar results.

*, $P < 0.05$; ***, $P < 0.001$

Figure 2. NTPX2 and NPTXR drive the mutual interaction between NB and microenvironment cells. (**A**) Fluorescent NB cells were mixed with HUVECs and grown to confluence in the presence of CTRL or NPTX2/NPTXR-targeting agents. Fluorescent areas were quantified with ImageJ and have been processed in reverse-mode to be visualized in black. NB cells were evaluated for their adhesion on confluent layers of HUVECs, HMECs or HBPV cells in the same conditions as in **A**; adhered cells were counted with ImageJ (**B**). Migration of SH-SY5Y cells towards HUVECs, HMECs or HBPV cells (5×10^4/well) was evaluated in a transwell system in the same conditions as in **A**; migrated cells were stained with crystal violet and counted under a light microscope (**C**). Graph bars represent mean ± S.D. from triplicate points of two independent experiments.
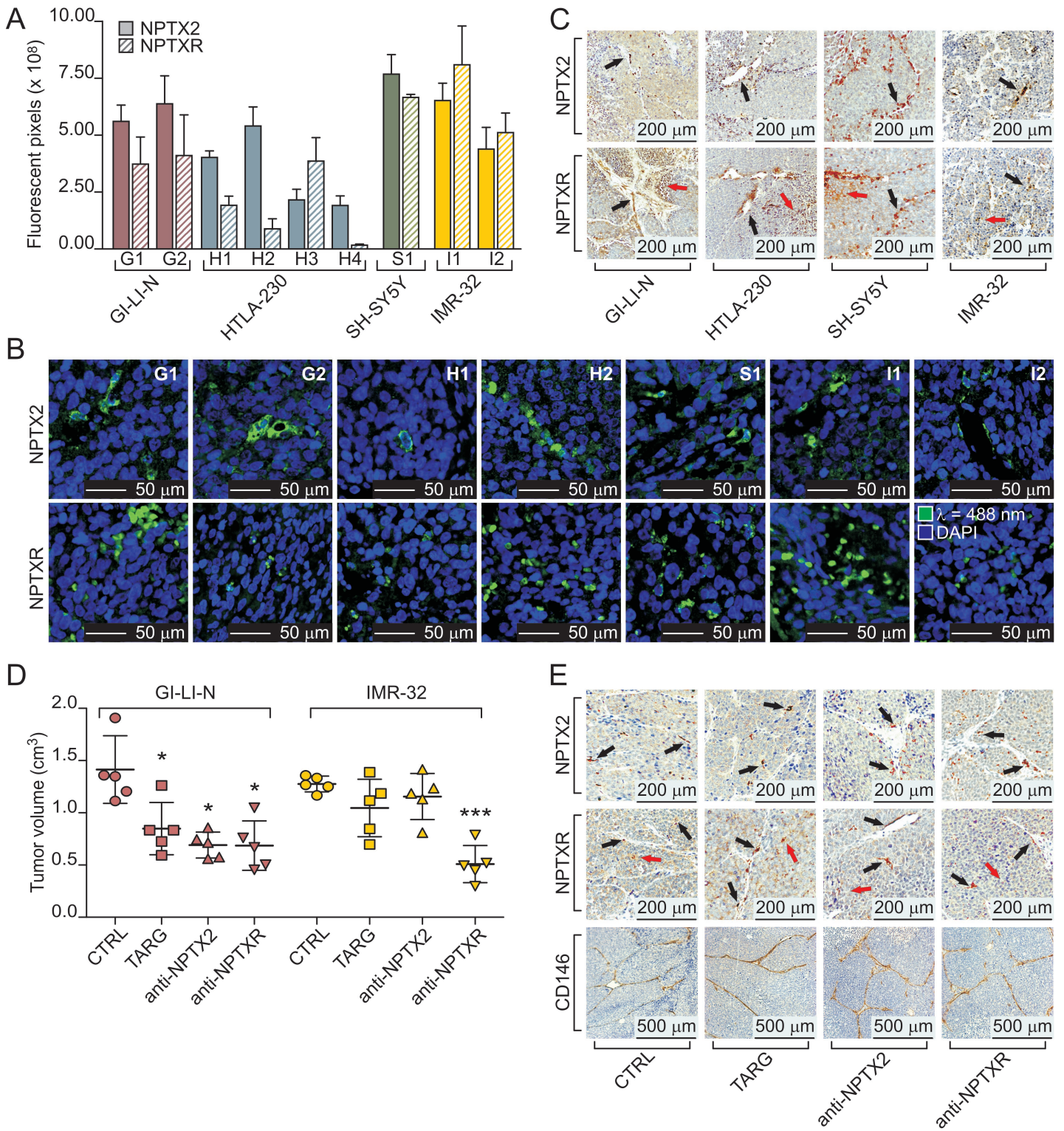
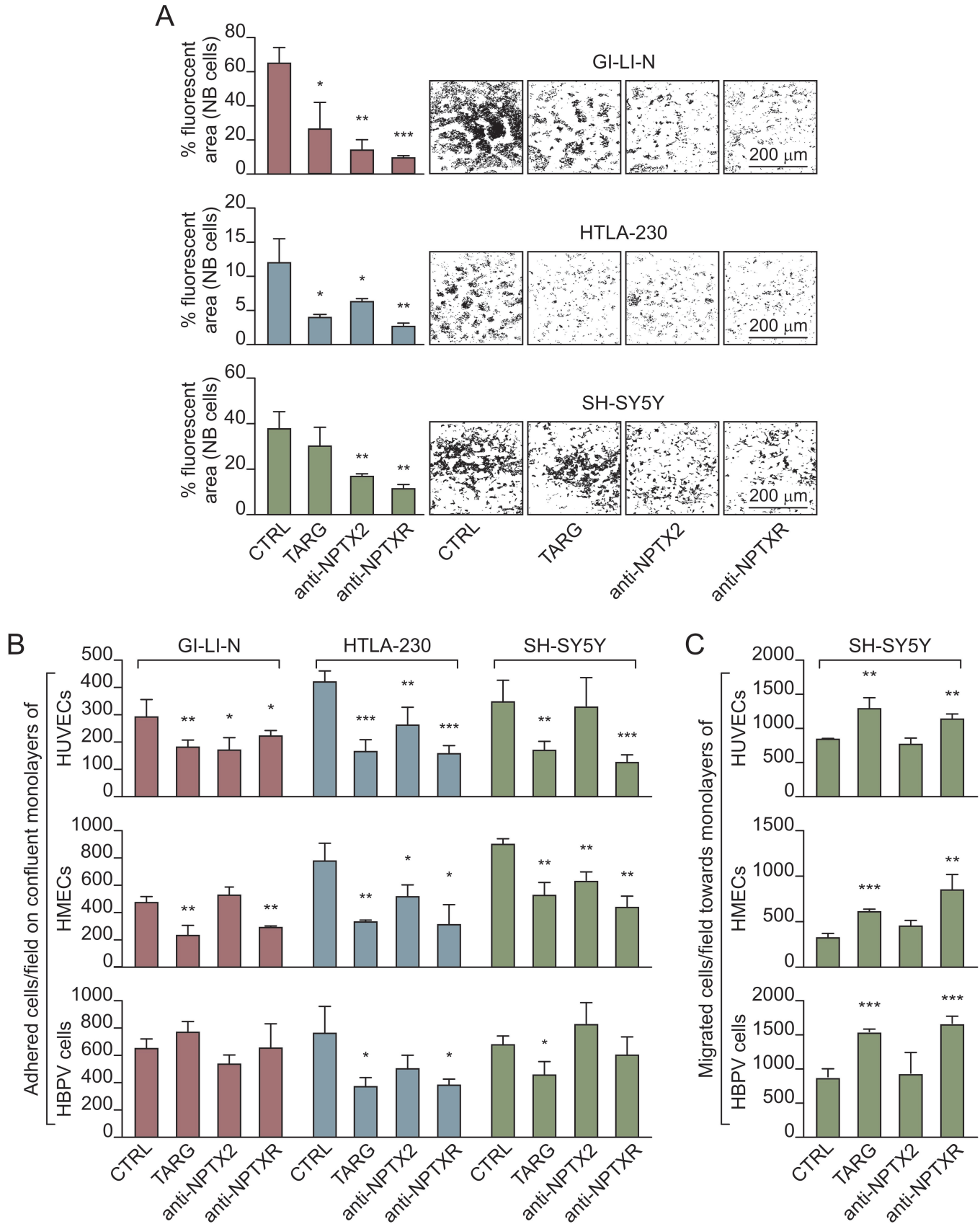*, $P < 0.05$; **, $P < 0.01$; ***, $P < 0.001$

14

Figure 3. NPTX2 and NPTXR are expressed in human NB, where NPTX2 is a prognostic marker of poor outcome. IF and IHC staining of human specimens were performed as described in Fig. **1**. Patient IDs: Patient #1, 07-B-1173 A1; Patient #2, 07-B-1312 A2; Patient #3, 07-B-1617 A2. Representative tissue staining is shown. White arrows, blood vessels; red arrows, tumor cells (**A**). The correlation between NPTX2, NPTXR and VE-cadherin expression and clinical outcomes in NB patients was evaluated on the SEQC dataset (**B**).
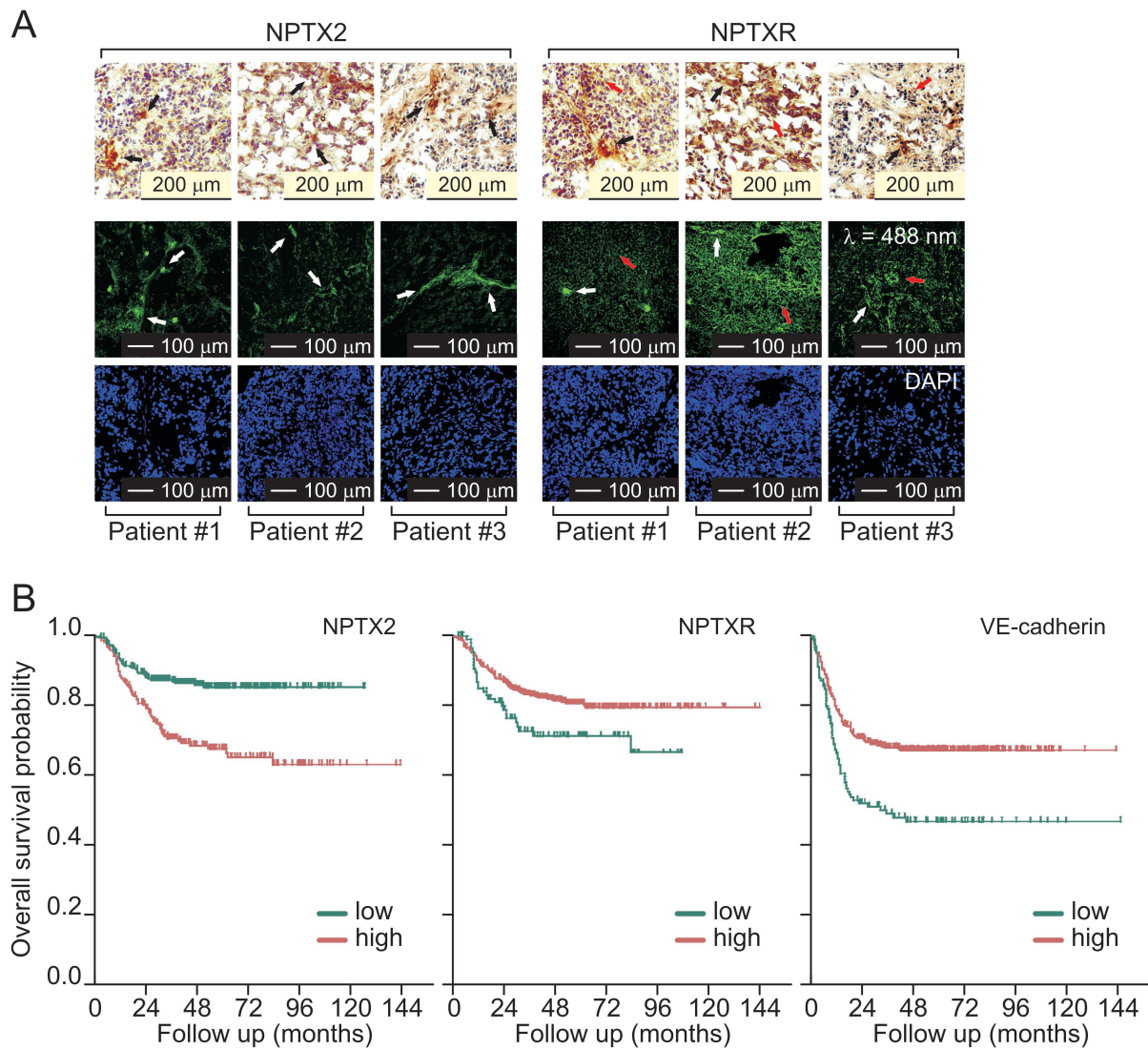
X^2 = 21.70; *P* = 3.2 × 10^{-6} (**NPTX2**); X^2 = 5.48; *P* = 0.019 (**NPTXR**); X^2 = 16.07; *P* = 6.1e-05 (**VE-cadherin**)
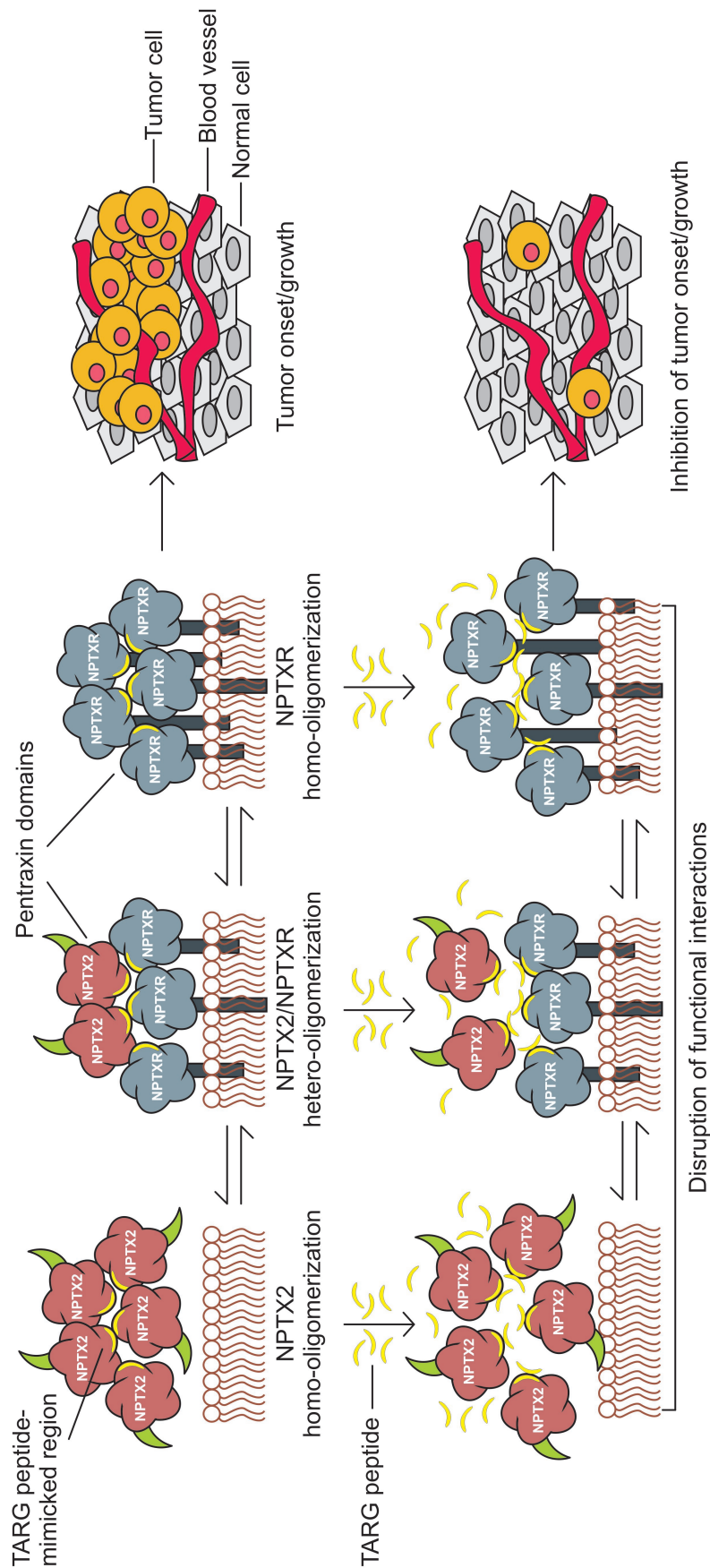
Figure 4. The targeting of NPTX2 and NPTXR inhibits NB. A highly conserved pentraxin domain is present in both NPTX2 and NPTXR, mediating homo- and hetero-oligomerization (likely, pentamerization) of these proteins. The NPTX2/NPTXR pathway is responsible for the reciprocal recognition between normal microenvironment cells and neuroblasts that promotes NB onset and progression. In the presence of a targeting agent, such as the TARG peptide, these interactions are disrupted, resulting in the inhibition of tumor onset and progression.

15

Bartolini et al., Figure 1

Bartolini et al., Figure 2

A

B

Bartolini et al., Figure 3

Bartolini et al., Figure 4

Cancer Research

The Journal of Cancer Research (1916–1930) | The American Journal of Cancer (1931–1940)

AACR American Association for Cancer Research

The neuronal pentraxin-2 pathway is an unrecognized target in human neuroblastoma which also offers prognostic value in patients

Alice Bartolini, Daniela Di Paolo, Alessio Noghero, et al.

Updated version	Access the most recent version of this article at: doi:10.1158/0008-5472.CAN-15-0649
Supplementary Material	Access the most recent supplemental material at: http://cancerres.aacrjournals.org/content/suppl/2015/08/20/0008-5472.CAN-15-0649.DC1.html
Author Manuscript	Author manuscripts have been peer reviewed and accepted for publication but have not yet been edited.

E-mail alerts	Sign up to receive free email-alerts related to this article or journal.
Reprints and Subscriptions	To order reprints of this article or to subscribe to the journal, contact the AACR Publications Department at pubs@aacr.org.
Permissions	To request permission to re-use all or part of this article, contact the AACR Publications Department at permissions@aacr.org.